Electrowetting lenses for compensating phase and curvature distortion in arrayed laser systems

Robert D. Niederriter,[1,*] Alexander M. Watson,[2] Ramzi N. Zahreddine,[3] Carol J. Cogswell,[3] Robert H. Cormack,[3] Victor M. Bright,[2] and Juliet T. Gopinath[3]

[1]Department of Physics, University of Colorado—Boulder, 390 UCB, Boulder, Colorado 80309, USA

[2]Department of Mechanical Engineering, University of Colorado—Boulder, 427 UCB, Boulder, Colorado 80309, USA

[3]Department of Electrical and Computer Engineering, University of Colorado—Boulder, 425 UCB, Boulder, Colorado 80309, USA

*Corresponding author: robert.niederriter@colorado.edu

Received 19 February 2013; revised 9 April 2013; accepted 10 April 2013; posted 10 April 2013 (Doc. ID 185479); published 7 May 2013

We have demonstrated a one-dimensional array of individually addressable electrowetting tunable liquid lenses that compensate for more than one wave of phase distortion across a wavefront. We report a scheme for piston control using tunable liquid lens arrays in volume-bound cavities that alter the optical path length without affecting the wavefront curvature. Liquid lens arrays with separately tunable focus or phase control hold promise for laser communication systems and adaptive optics. © 2013 Optical Society of America

OCIS codes: (220.1080) Active or adaptive optics; (220.3630) Lenses; (230.4685) Optical microelectromechanical devices.

http://dx.doi.org/10.1364/AO.52.003172

1. Introduction

Liquid lenses have received considerable attention for the ability to provide variable focus in optical systems, enabling the advancement of optical communication, cameras, display technology, and wavefront compensation in general. Robust, compact, highly tunable liquid lenses with fast response times on the order of 1 ms have been demonstrated based on the electrowetting effect [1–5], wherein an applied voltage shapes the curvature of a conducting liquid droplet. The same principle can be combined with multiple electrodes addressing a single lens element to realize liquid prisms for beam steering capability [6–8].

Electrowetting lenses and prisms can provide improvements over other methods of wavefront control, such as spatial light modulators, deformable mirrors, and MEMS mirrors. Advantages of electrowetting technology include polarization insensitivity, fast response, and the ability to operate in transmission rather than in reflection geometry. Furthermore, electrowetting solutions to wavefront distortion problems are attractive due to the versatility of the liquid interface, which can be adapted to adjust curvature with variable focus, tip-tilt with liquid prisms, and, as we demonstrate in this report, phase delay (piston) by altering the optical path length.

Realizing the great potential of electrowetting devices for wavefront control requires arrays with individually addressable elements. While there have been recent developments in creating two-dimensional electrowetting arrays with fill-factor as high as to 90% [7], the fabrication that would allow individually addressable elements remains a challenge. However, one-dimensional arrays of electrowetting lenses provide solutions for practical applications, such as correcting for misalignment in laser arrays, as demonstrated in this paper.

1559-128X/13/143172-06$15.00/0

We report on a linear array of focus-tunable electrowetting lenses, as well as the novel capability to compensate phase distortion over a full wavelength in a transmission optical system. A liquid lens placed at the focus between fixed lenses allows piston to be controlled independent from curvature. The experiment in this paper validates the proposed phase control scheme simulated in [9]. To the best of our knowledge, this is the first demonstration of piston control using an electrowetting device operating in transmission. We also propose a direct application of one-dimensional electrowetting lens arrays for compensating axial misalignment in laser arrays and report preliminary results. This work demonstrates the potential of individually addressable electrowetting lens arrays to impact optical systems by adjusting both curvature and piston.

2. Fabrication Methods

The electrowetting effect describes how an applied voltage between a conductive liquid droplet and substrate determines the contact angle of the droplet [10]. Electric charge buildup at the interface increases the surface energy, pulling the liquid close to the surface and reducing the contact angle. The contact angle in turn determines the liquid curvature, and therefore directly affects the focal length of the lens formed at the spherical droplet surface. To prevent hydrolysis, a dielectric layer is inserted between the substrate electrode and liquid. Using a hydrophobic dielectric surface increases the initial contact angle, enabling a greater range of focal tuning. Achieving lens tuning requires fabricating a structure with electrodes, a dielectric layer, and a hydrophobic surface.

The individually addressable array of lenses was formed within a three-chip stack consisting of a bottom glass slide with patterned indium-tin oxide (ITO) electrodes, a silicon middle layer with cavity walls defined by potassium hydroxide (KOH) through etch, and a top cover glass to contain the liquids, as shown in Fig. 1. We designed a one-dimensional array with separately controlled elements to show proof of concept for lens arrays that are able to compensate wavefront distortion and axial misalignment in laser arrays. While KOH etches silicon in smooth planes crucial to electrowetting, the sloped sidewalls prevent high fill-factor. Low fill-factor, one-dimensional arrays simplify fabrication and are sufficient for our demonstration of compensating for axial misalignment in linearly arrayed laser fibers. Two-dimensional, high fill-factor arrays benefit many applications, and previously demonstrated fabrication methods provide a means to achieve these in future designs [4,7]. To increase fill factor, the cavity sidewalls should be as vertical as possible and circular lenses should be arrayed in a hexagonal format, suggesting a photo-definable polymer layer may be best suited for future liquid cavities. The issue of separately addressing each element in such an array poses a challenge when array pitch is increased. Future designs can utilize through-wafer interconnects, allowing the leads to fan out without contact to the liquids in the cavity.

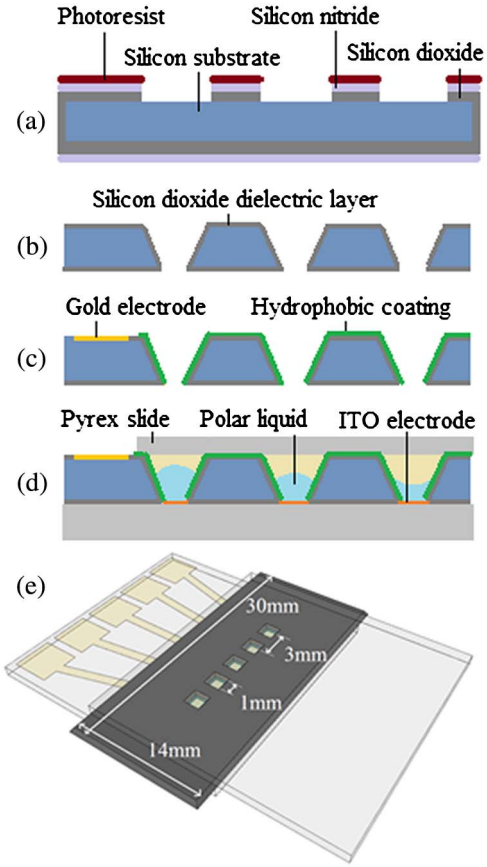

Fig. 1. Liquid lens array fabrication process. (a) Silicon dioxide was thermally grown, silicon nitride was deposited by PECVD process, photoresist was lithographically patterned, and buffered oxide etch exposed the silicon. (b) A wet KOH etch through the silicon created the cavities to hold the liquid lenses with 1 mm^2 apertures. Thermal oxide was regrown as the dielectric layer. (c) The sample was shadow masked and exposed to reactive ion etching to make electrical contact to the substrate for Ti/Au electrode deposition. A hydrophobic fluorocarbon polymer (C_4F_8 gas precursor) was deposited on the substrate within an ICP system. (d) The arrays were then bonded onto glass slides with patterned ITO electrodes. After filling the cavities with the conducting and nonconducting liquids, the device was capped with a Pyrex slide. (e) The assembled lens array device (to scale). Note that due to the anisotropic nature of the KOH etch, the minimum aperture size is 1 mm^2 and occurs on the bottom side of the silicon.

The fabrication process began with double side polished 500 μm thick, 76.2 mm diameter *n*-doped (100) silicon wafers, which serve as the common electrode (10–30 Ω cm resistivity). To protect the silicon through the aggressive KOH etch, 250 nm of silicon dioxide (SiO_2) was thermally grown and 550 nm of low stress silicon nitride (Si_3N_4) was deposited on both sides of the wafer using plasma-enhanced chemical vapor deposition (PECVD) [11]. Photolithography was used to define the 1 mm^2 square apertures for the lens array. A buffered oxide etch was used to expose the silicon to allow the KOH etch to define the lens cavities. The wafer was submerged

in 40% KOH at 70°C and allowed to etch until completion. This wet etch was chosen because it yields extremely smooth sidewalls, which reduce the effects of contact angle pinning and hysteresis [3]. After the KOH etch, the remaining SiO_2 and Si_3N_4 layers were removed with another buffered oxide etch.

Next, the dielectric layer of 250 nm silicon dioxide was thermally grown at 1100°C in a hydrogen and oxygen environment. Thermal oxide was chosen because it is pinhole-free down to nanometer thicknesses [12], ensuring minimal current leakage during operation. The wafers were masked and processed in a reactive ion etch to expose the silicon near the edge of the sample. This was immediately followed by a thermal evaporation of 15 nm titanium and 85 nm of gold. For the final processing step with the silicon substrate, a hydrophobic layer was deposited on top of the dielectric. Two hydrophobic layers were used separately in this study: Teflon AF and a Teflon-like fluoropolymer commonly used as the passivation layer in the Bosch process [13]. Teflon AF was dip-coated from a 10:1 solution of Fluorinert FC-77: DuPont Teflon AF 1600 and baked above its glass transition temperature at 170°C. The Teflon-like fluoropolymer was deposited in an ICP system. A C_4F_8 precursor gas was introduced to yield a 20 nm thin polymer hydrophobic layer. This vapor-phase deposition produced a uniform hydrophobic layer suitable for use with electrowetting systems [3].

We have analyzed the threshold for capillary action, which would allow water to wet to the top of the cavities and cause device failure. The critical contact angle, calculated to be 35° from the Concus–Finn relation [14], cannot be reached before contact angle saturation at 70°. Thus, electrowetting contact angle saturation limits our system performance rather than capillary action.

3. Electrowetting Lens Arrays

Each lens in the array receives a separate voltage through the patterned ITO electrodes. Tuning was achieved by applying a 5 kHz AC square wave to the electrode. AC voltage was chosen to reduce contact angle hysteresis by minimizing charging of the dielectric. For the initial experiments measuring change in focal length and lens aberrations of single lenses, a blank Pyrex glass slide was anodically bonded to the bottom of the silicon device layer at 1500 V and 300°C for approximately 6 h. Trimethyl-siloxy-terminated poly(dimethylsiloxane) silicone oil (Gelest DMS-T11, hereafter referred to as *silicone oil*) and deionized water with 1% SDS surfactant (Alfa Aesar A11183, hereafter called *SDS solution*) were chosen as the nonpolar and polar liquids, respectively. The surfactant was chosen to reduce the surface tension between the water and oil such that the voltage required to adjust the contact angle is further reduced [15]. Silicone oil was chosen for low viscosity and nearly the same density as water (density difference 0.07 g/mL). A micropipette was used to deposit liquids into the lens cavities. The top glass with patterned ITO electrodes was aligned and clamped onto the filled silicon chip to complete the device for lens characterization and focal length tuning.

Testing the individually addressable lens elements required bonding the electrode-patterned glass onto the bottom of the stack to avoid potential shorts between cavities caused by the conductive liquid trapped between the top glass and the silicon. Since the ITO is not secured by the anodic bonding process, a different approach was implemented to secure the glass to the substrate. Aperture holes were cut into double-sided kapton tape, and the silicon, tape, and glass were aligned under a microscope and pressed together to bond. The conducting liquid chosen for this test was a 1:1 mixture of Cargille immersion liquids OHZB and OHGL (Cargille Labs 19580 and 19581). These were chosen for higher index contrast to clearly depict the individual focal length tuning, and for higher viscosity to mitigate liquid leakage through the porous tape bond.

4. Lens Characterization

Focal length tuning was measured by passing a He–Ne laser beam through the liquid lens and recording the spot size on a wavefront sensor. Using SDS solution and silicone oil as the lens liquids, optical power is tunable from -29 to -34 m^{-1} (-30 to -34 mm focal lengths), limited to low voltages by hydrolysis at the sharp edges of the etched cavity. The patterned electrodes allow separate tuning of each lens' focal length, as shown in Fig. 2. At first no voltage is applied, followed by separate tuning of the middle and left lenses with 17 V_{rms} and 20 V_{rms}, respectively. Finally, the voltage was removed and the lenses return to their original focal lengths. The individual tuning demonstrated here is essential for correcting each element of a laser array.

One direct application of a one-dimensional array of separately tunable lenses is correcting for misalignment in laser arrays. This is compatible with arrays of manually aligned fibers and the misalignment laser diode arrays undergo during packaging, referred to as "smile" [16]. A bend in the laser array results in emitters that are offset along or transverse to the optical axis. Standard fixed microlens arrays cannot simultaneously collimate the light from axially misaligned elements. Smile is a costly problem that reduces the usable laser power and typically requires a custom lens array or phase plate to match the bending of the diode array [17,18]. Prism arrays can compensate for transverse smile and individually addressable electrowetting lens arrays can correct the axial component.

We have used our lens array for preliminary demonstrations of the axial misalignment. Laser light at 980 nm was coupled into an array of four single-mode fibers mounted in a *v*-groove array to imitate an array of laser sources, with ~1 mm misalignment along the optical axis. A lens array was positioned about

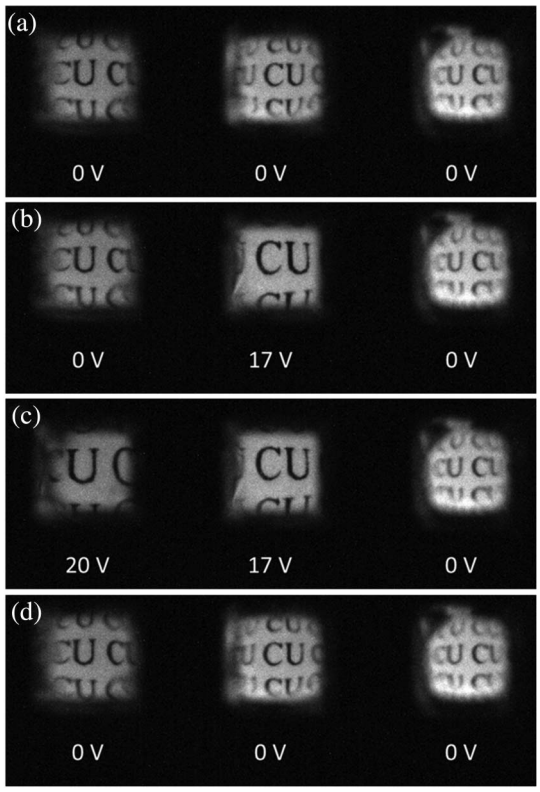

Fig. 2. Sequence of images demonstrating separately tunable adjacent lenses. This three-lens array used Teflon AF as the hydrophobic layer and the mixture of Cargille OHZB and OHGL as the conducting liquid. Circular pinhole apertures (~1 mm diameter) were aligned beneath the lens array to reduce image distortion from the square corners. Viewed through the lens array is a printed page of our university's acronym, CU, each letter measuring 1.3 mm in height. (a) No voltage applied to any of the lenses; (b) 17 V_{rms} applied to the center lens; (c) 20 V_{rms} applied to the lens on the left, 17 V_{rms} applied to the center lens; and (d) no voltage applied to any of the lenses, showing they return to their original focal lengths, as in (a), with little or no hysteresis.

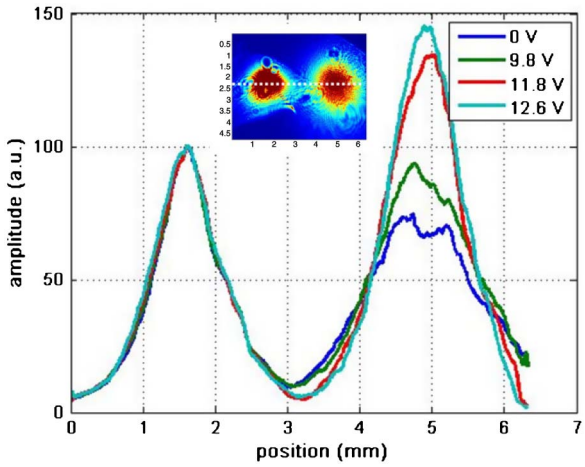

Fig. 3. Measurement of laser intensity as a function of position on CCD camera along a reference axis shown as the dotted white line. The first peak represents the left laser source and the second represents the source on the right. The two laser fiber sources were axially misaligned by ~1 mm. By adjusting the focus of the lens on the right, the corresponding spot size was corrected. For this particular pair of misaligned laser sources, ~11 V was applied to the right liquid lens to match the spot sizes. The inset shows the two spots with no applied voltage, with a line indicating the cross section plotted.

2 mm from the end of the fiber array, and a CCD camera was used to collect the focused light. We tuned the lens focal lengths to alter the beam widths from as large as 1.9 mm to match a 1.1 mm reference diameter, correcting for millimeter-scale axial misalignment of the individual fibers. Figure 3 below shows a cross section of irradiance as a function of position. As the focal length of the lens on the right was adjusted, the spot size and therefore irradiance pattern along the reference line were altered. These particular fibers were misaligned by ~1 mm but the spot sizes from the fiber array were matched by applying ~11 V to one of the lenses. The inset shows the two spots with no applied voltage, slightly distorted by the imperfections in the circular apertures used to avoid the square edges of the lenses. Using lower numerical aperture fibers would reduce diffraction effects from the edges of the lens array and improve the beam quality.

Lens quality is vital for many applications. To measure the lens aberration, a spatially filtered 532 nm laser beam was passed through the 1 mm^2 lens aperture and expanded 2.5 times to fill the input of a Wavefront Sciences μ-eye Shack–Hartmann wavefront sensor. The lens had a vapor-phase fluoropolymer coating and was filled with silicone oil and SDS solution. The wavefront emerging from the lens was measured to have 550 nm rms deviation from a spherical wavefront. Much of this error is due to the square corners of the lens, where the liquid surface is not expected to be spherical. Including a 1 mm diameter circular aperture matching the lens size, the rms wavefront deviation is only 80 nm. This compares favorably to the literature where, for comparison, a 1 mm diameter solid microlens was shown to have 79.25 nm rms wavefront error [19], and a similar square liquid lens was measured to have 211.16 nm rms deviation (using a similar circular aperture) [20]. To further characterize the lens quality, we fitted the wavefront to Zernike polynomials and have listed five of the fitted Zernike coefficients in Table 1. In particular, we measure an order of magnitude less spherical aberration, but approximately twice as much astigmatism than [20] with a similar square electrowetting microlens. These aberrations lead to rms wavefront variation of $\lambda/12$ over the 100 μm diameter center of the lens,

Table 1. Measured Zernike Coefficients of Microlens

Aberration	Zernike Coefficient (μm)
Astigmatism 90°	0.445
Astigmatism 45°	0.4997
Coma x	−0.0439
Coma y	0.0282
Spherical aberration	−0.0324

sufficiently small enough to justify using the lens array as a phase modulator as demonstrated in the following section. While we have measured the lens quality without applied voltage, we do not expect a significant change in quality during tuning. The change in spherical aberration with lens tuning was modeled numerically based on the methods of [21]. We calculated the spherical aberration to be small in every tuning condition, increasing from $-0.017\ \lambda$ in the resting state to $-0.011\ \lambda$ with 5 V applied.

5. Piston Control

Piston control in optical systems is a powerful tool for applications like coherent combining, pulse synthesis, and wavefront control. The tunable liquid lenses described in this paper can be used to control piston independently from curvature [9], whereby the varifocal lens array is placed at the focal point of a fixed lens array telescope with the same pitch. Figure 4(a) shows the piston control scheme. By focusing the incident light onto the liquid lens interface, piston can be adjusted with minimal effect on the wavefront. Because the liquids within the cavity are constrained by constant volume, the center position of the oil–water boundary shifts as the lens is tuned. Passing through more oil increases the optical path length (OPL) and therefore changes the phase of the light exiting the liquid lens.

While the wavefront curvature is unchanged due to a tight focus at the interface of the liquid lens, the tip/tilt could be affected if the optical axis of the electrowetting lens is unstable. The main cause of axis instability in electrowetting lenses is gravitational pull causing deformation of the spherical lens shape due to slightly mismatched liquid densities. Gravitational deflection shifts the liquid lens optical axis away from the center. Simulations have shown that gravity plays a negligible role in the lens shape for lens diameters smaller than 2 mm, taking into account the density difference between the silicone oil and SDS solution used in this work. This lens design produces the optical axis stability necessary for the demonstrated piston adjustment technique.

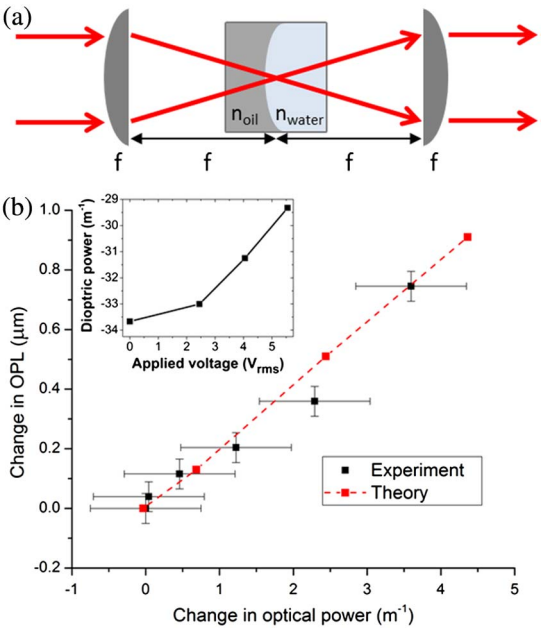

Fig. 4. (a) Schematic for piston control using a tunable lens at the focus of a telescope (not to scale). (b) Measured change in optical path length (OPL) through the liquid lens with AC voltage applied. Measured change (experiment) is compared to that predicted by a Zemax model of the lens, using independent measurements of the optical power (theory), inset. This lens used a Teflon AF hydrophobic layer, with silicone oil and SDS solution as the lens liquids.

We have verified experimentally that a tunable liquid lens placed at the focus of two fixed-focus lenses can be used to manipulate the piston. We used a He–Ne laser (633 nm) in a Mach–Zehnder interferometer with the fixed/tunable/fixed lens combination shown in Fig. 4(a) occupying one arm. The fixed-focus lenses were chosen with focal length of 50 mm such that the Rayleigh range was greater than the thickness of the liquid lens (0.5 mm), ensuring a narrow beam passing through the tunable lens.

A CCD camera recorded the interference fringes. Motion of one optical fringe corresponds to a change in OPL of one wavelength. Figure 4(b) shows the average variation of OPL as the liquid lens was tuned. The interferometer measures the phase change as a function of position across the wavefront. The phase change deviates by ~5% across the entire wavefront, which justifies displaying the spatial average in Fig. 4(b). Zemax was used to model the expected piston change. The two liquid volumes are held constant while the curvature of the boundary is changed to simulate the effects of electrowetting. The measurements and predictions agree well. We expect small deviations between individual lenses in an array to be corrected by operating the voltage control within a simple feedback loop. In practice, less than one wave of piston control ($\lambda \sim 0.5$ μm for visible light) is usually needed for beam correction, and these results show that more than one wave of control is possible with our tunable lenses. Thus, this system could be extended to arrays of individually addressable liquid lenses mounted at the focal plane between standard fixed-focus lens arrays to provide piston-compensation for adaptive optics systems.

Coaxial alignment of three lens arrays of this size can be achieved with standard optical alignment tools. A compact system could be constructed using short focal length lens arrays combined into a single packaged device with the electrowetting lens array. Standard lens arrays are available with focal lengths of 5 mm, enabling a device ~10 mm thick.

Pixilated elements are a common issue to all methods of adjustable piston compensation. By utilizing challenging fabrication methods, spatial light modulators, deformable mirrors, and segmented mirrors achieve high fill factors that minimize the problems of pixilation. The piston compensation method based

on electrowetting lenses more readily achieves high effective fill factor by nature of the three-lens optical system. Light for each "pixel" is collected by the fixed lens elements with sizes matched to the pitch of the electrowetting lens array. The effective fill factor is that of the fixed lens array used to concentrate light into the center of each liquid lens. Such fixed lens arrays can be made with high fill factor, even to 100% [22].

The Zemax model of the system predicts less than 3 nm rms wavefront distortion due to the liquid lens, independent of lens curvature. Experimentally, we observed no change in laser beam divergence when inserting the liquid lens at the focus, confirming this method can modify piston independent of wavefront curvature.

6. Conclusion

We have designed and fabricated linear arrays of individually tunable electrowetting liquid lenses and demonstrated their capability for correcting piston and curvature in adaptive optics applications as well as compensating for axial misalignment in laser arrays. This marks the first time electrowetting technology has altered piston independent of wavefront curvature in a transmission optical system. Phase distortion of more than one wave can be corrected with tunable electrowetting lenses combined with fixed-focus lens arrays. Combining lens and prism arrays provides control of piston, tip-tilt, and curvature. Electrowetting devices provide three capabilities needed for advanced wavefront engineering. High fill factor is also necessary to achieve high-quality adaptive optical devices. Further investigations should focus on high fill-factor lens and prism arrays for applications such as smile compensation in diode laser arrays, coherent combining, and compensating for atmospheric distortion in communication and imaging.

The authors would like to acknowledge technical discussions with Keith Cobry (University of Colorado, Mechanical Engineering) and Joyce Wu (Qualcomm), support applying the hydrophobic coatings from Youngwoo Yi and Noel Clark (University of Colorado, Liquid Crystals Materials Research Center), and support in lens wavefront characterization from Robert McLeod and Chunfang Ye (University of Colorado, Electrical, Computer, and Energy Engineering). This work is sponsored by the 2011 Office of Naval Research Chief of Naval Research (CNR) Challenge Program, Award N00014-11-1-0574. This research was supported in part by the NNIN at the Colorado Nanofabrication Laboratory and the National Science Foundation under grant ECS-0335765. A. M. Watson received support from a Measurement Science and Engineering fellowship through the University of Colorado and the National Institute of Standards and Technology (NIST). R. D. Niederriter received support from the Department of Defense through the National Defense Science & Engineering Graduate Fellowship (NDSEG) Program.

References

1. B. Berge and J. Peseux, "Variable focal lens controlled by an external voltage: an application of electrowetting," Eur. Phys. J. E **3**, 159–163 (2000).
2. S. Kuiper and B. H. W. Hendriks, "Variable-focus liquid lens for miniature cameras," Appl. Phys. Lett. **85**, 1128–1130 (2004).
3. F. Krogmann, W. Mönch, and H. Zappe, "A MEMS-based variable micro-lens system," J. Opt. A **8**, S330–S336 (2006).
4. N. R. Smith, L. Hou, J. Zhang, and J. Heikenfeld, "Fabrication and demonstration of electrowetting liquid lens arrays," J. Disp. Technol. **5**, 411–413 (2009).
5. I. Voitenko, R. Storm, R. Westfall, and S. Rogers, "Interferometric control of contact line, shape, and aberrations of liquid lenses," Proc. SPIE **6714**, 67140J (2007).
6. N. R. Smith, D. C. Abeysinghe, J. W. Haus, and J. Heikenfeld, "Agile wide-angle beam steering with electrowetting microprisms," Opt. Express **14**, 6557–6563 (2006).
7. L. Hou, J. Zhang, N. Smith, J. Yang, and J. Heikenfeld, "A full description of a scalable microfabrication process for arrayed electrowetting microprisms," J. Micromech. Microeng. **20**, 015044 (2010).
8. Y. Takai, R. Koshiishi, S. Kirita, M. Tsuchiya, Y. Watanabe, K. Takahashi, Y. Imai, and Y. Shimpuku, "Electrowetting Fresnel lenticular," in *Proceedings of the IEEE International Conference on Micro Electro Mechanical Systems* (IEEE, 2012), pp. 632.
9. J. T. Gopinath, V. M. Bright, C. C. Cogswell, R. D. Niederriter, A. Watson, R. Zahreddine, and R. H. Cormack, "Simulation of electrowetting lens and prism arrays for wavefront compensation," Appl. Opt. **51**, 6618–6623 (2012).
10. F. Mugele and J.-C. Baret, "Electrowetting: from basics to applications," J. Phys. Condens. Matter **17**, R705–R774 (2005).
11. H. Seidel, L. Csepregi, A. Heuberger, and H. Baumgartel, "Anisotropic etching of crystalline silicon in alkaline solutions," J. Electrochem. Soc. **137**, 3612–3626 (1990).
12. A. J. Niskanen, T. Ylinen-Hinkka, S. Kulmala, and S. Franssila, "Ultrathin tunnel insulator films on silicon for electrochemiluminescence studies," Thin Solid Films **517**, 5779–5782 (2009).
13. M. J. Madou, *Fundamentals of Microfabrication* (CRC Press, 2002).
14. P. Concus and R. Finn, "On the behavior of a capillary surface in a wedge," Proc. Natl. Acad. Sci. USA **63**, 292–299 (1969).
15. S. Berry, J. Kedzierski, and B. Abedian, "Low voltage electrowetting using thin fluoropolymer films," J. Colloid Interface Sci. **303**, 517–524 (2006).
16. J. Wang, Z. Yuan, L. Kang, K. Yang, Y. Zhang, and X. Liu, "Study of the mechanism of "smile" in high power diode laser arrays and strategies in improving near-field linearity," in *Proceedings of IEEE Electronic Components and Technology Conference* (IEEE, 2009), pp. 837–842.
17. C. E. Hamilton, S. C. Tidwell, D. Meekhof, J. Seamans, N. Gitkind, and D. D. Lowenthal, "High-power laser source with spectrally beam-combined diode laser bars," Proc. SPIE **5336**, 1–10 (2004).
18. J. F. Monjardin, K. M. Nowak, H. J. Baker, and D. R. Hall, "Correction of beam errors in high power laser diode bars and stacks," Opt. Express **14**, 8178–8183 (2006).
19. P. Nussbaum, R. Völkel, H. P. Herzig, M. Eisner, and S. Haselbeck, "Design, fabrication and testing of microlens arrays for sensors and microsystems," Pure Appl. Opt. **6**, 617–636 (1997).
20. F. Krogmann, W. Mönch, and H. Zappe, "Electrowetting for tunable microoptics," J. Microelectromech. Syst. **17**, 1501–1512 (2008).
21. S.-L. Lee and C.-F. Yang, "Numerical simulation for meniscus shape and optical performance of a MEMS-based liquid micro-lens," Opt. Express **16**, 19995–20007 (2008).
22. Holographix, LLC.